LNF-98/009

Determination of Local Structure in Monofase Palladium by X–Ray Absorption Spectroscopy

F. Boscherini, S. de Panfilis, J. Wissmüller

Physical Review. B, 57, 6, 3365–3374, (1998)

Determination of local structure in nanophase palladium by x-ray-absorption spectroscopy

F. Boscherini* and S. de Panfilis†
INFN, Laboratori Nazionali di Frascati, P.O. Box 13, I-00044, Frascati (Rome), Italy

J. Weissmüller
Technische Physik, Universität des Saarlandes, P.O. Box 15 11 50, D-66041 Saarbrücken, Germany
(Received 20 June 1997)

We report a comprehensive investigation of nanophase palladium by x-ray-absorption spectroscopy with the aim of clarifying the issue of the structure of the grain boundaries in nanophase materials. In fact, since the proposal that the grain boundaries in these materials are highly disordered, various techniques have obtained conflicting results on this issue. Until two recent brief reports (one of which was our own) x-ray-absorption spectroscopy investigations have supported the view of highly disordered grain boundary regions due to the finding of greatly reduced average coordination numbers. Contrary to previous reports we find that the reduction in average coordination numbers is smaller than previously reported (at most $4 \pm 0.03\%$ for the first shell) and can be explained by a size effect due to the non-negligible interface-to-bulk ratio of the samples. The analysis of the x-ray-absorption data has been extended up to the eighth coordination shell taking into account the important multiple-scattering paths. [S0163-1829(98)10001-2]

I. INTRODUCTION

The interest in the structure of nanophase (n) materials[1] originates from the high density of grain boundaries (GB's) present. Since GB's alter important physical properties of n materials,[2,3] knowledge of their local structure is clearly of great importance. Due to their high volume density it is feasible to investigate their properties with volume sensitive methods, which is impossible in ordinary coarse-grained samples. Also, investigation of GB's in n materials might provide insight on their structure in general, in n materials and in coarse-grained ones, and on the possible modifications with grain size.

An early x-ray-diffraction study[4] on nanophase Fe reported a large diffuse scattering background that was interpreted as arising from a structure having no long-range or short-range order in the GB; this was proposed to lead to a GB radial distribution function (RDF) lacking either short-range or long-range order and the term ''gaslike'' was used to describe the local atomic arrangement. However, the quantification of this ''disordered'' state has remained elusive. The fundamental feature of the proposed ''disordered'' model is the presence of atoms whose average position does not belong to the lattice of any of the adjacent crystallites and that have a low average coordination and/or a high disorder, leading to significant excess volume. In the following, for brevity, this type of arrangement will be described as ''disordered.'' For the sake of clarity it must be noted that the concepts of coordination number (CN) and disorder are completely separate. The CN counts the number of atoms in each coordination sphere, which is a well-defined concept when there is no overlap between peaks of the RDF; disorder can be quantified by the second and higher moments of each peak of the RDF, the leading term being the mean-square relative displacement (MSRD). Notwithstanding this, the single term ''disordered'' will be used in the following to describe the proposed structure for GB's in n materials.

The proposal of ''disordered'' GB's in n materials has been controversial with results from different techniques either supporting or rejecting this model. We note that also in studies rejecting ''disordered'' models of GB structure the conclusions are mainly qualitative, the principal conclusion being that the GB's are ''ordered'' or ''similar to those in conventional coarse-grained materials;'' a quantification of the degree of ''order'' is missing.

Among studies rejecting the ''disordered'' GB model is an x-ray-diffraction (XRD) study of n-Pd (Ref. 5) in which, contrary to the case of n-Fe, no diffuse scattering background was observed and only a peak broadening due to particle size and strain was detected. We note that the interpretation of XRD data has subsequently been challenged;[6] it was demonstrated that atomic correlations between atoms belonging to different randomly arranged crystallites do not give rise to diffuse scattering between the Bragg peaks as observed by Zhu *et al.*[4] and subsequently refuted by Fitzsimmons *et al.*[5] In this debate there have also been speculations on the degree of oxidation of n-Fe and on the different structure of GB's in fcc vs bcc metals.

TEM investigations have supported the ''ordered'' state of GB's.[7] We note, however, that TEM has limited atomic scale resolution and requires sample preparation procedures that may affect the GB structure itself. Also, the conclusion of the quoted TEM study is that ''any atomic displacement is less than or equal to 12% of the nearest-neighbor (NN) distance''; in fact, atomic displacements as large as 12% of the NN distance can only be classified as exceedingly large and such a situation could only be described as ''disordered,'' a fact that was apparently not recognized by the authors.

X-ray or neutron small-angle scattering measurements have remained inconclusive. In fact, spectra by Jorra *et al.*[8] have been fitted by a sum of contributions from ordered crystallites and from ''incoherent'' interfaces, while Sanders *et al.*[9] find no evidence at all of any signal originating from

0163-1829/98/57(6)/3365(10)/$15.00

the GB's and the excess small-angle signal is proposed to originate from voids.

Mössbauer studies of n-Fe have detected a signal attributed to the grain-boundary component;[10] the assignment was supported by the enhanced isomer shift (indicating a reduced atomic density) and by the enhanced width (indicating a more disordered structure relative to the bulk). Recently,[11] the same technique has provided evidence for enhanced compressibility of the grain-boundary component of n-Fe. Finally, positron lifetime measurements by Schäfer[12] provide evidence for vacancylike free volume at GB's and are thus in support of the presence of ''disordered'' GB's.

Computer simulations of GB structure have the advantage that the RDF can be extracted from the atomic positions, which is impossible for any experimental technique. Wolf and Lutsko[13] have studied a ''GB superlattice'' of Cu that consists of a regular array of twist boundaries, all of the same type and perpendicular to the (001) planes. The RDF that they calculate indicates that there are significant atomic relaxations at the GB. In fact, the RDF exhibits very broadened peaks indicating considerable disorder. Wolf[14,15] has studied in detail a number of GB's on the four densest planes of fcc metals in bicrystals. Also in this case the RDF of atoms at the GB plane exhibit considerably broadened peaks. Results of a computer simulation study of a model nanocrystalline material substantiate this conclusion.[16]

The latest study of local order in n materials by x-ray diffraction[17] provides evidence that in most samples studied a reduced CN in the first eight coordination shells is found but that this is due to a size effect, i.e., to the high interface-to-bulk ratio (IBR) of the sample with no evidence of further reduction due to ''disordered'' GB's; the GB's are described as nonreconstructed and incoherent, terms that will be better defined in the following. In freshly prepared samples, however, the same study found approximately 10% of atoms in positions that cannot be associated with any crystallite.

X-ray absorption spectroscopy (XAFS) (Ref. 18) has played an important role in this debate.[19] This is not surprising as XAFS is nondestructive, can directly measure local order parameters such as CN and MSRD, and has a relatively straightforward interpretation (at least as far as the dominant low-frequency signal is concerned). All measurements published before November 1995 have shown a large reduction of average CN's in the first few coordination shells; by using order-of-magnitude estimates of the particle size from XRD line broadening it was concluded that this reduction was greater than that compatible with a simple estimate of the IBR and most measurements were interpreted as compatible with the disordered GB model or with the presence of a high defect density.[20] The XAFS *technique* was therefore seen to support the ''disordered'' GB model.

The last two XAFS papers published on n materials have, however, completely changed this situation. Our group[21] published high quality data on n-Pd and provided an analysis of the first coordination shell demonstrating that only a small, if any, reduction in CN's is in fact observed and that this reduction can be simply explained by a size effect due to the high IBR; previous results were shown to be in error due to sample thickness inhomogeneities (an experimental artifact). At the same time Stern *et al.*[22] published a similar study on n-Cu that concluded that the average first-shell CN was not significantly different from the value in the ideal fcc structure; grain boundaries in n materials were thus proposed to be ''ordered.''

The purpose of the present paper is to describe in more detail our work, discuss in more depth the possible models of GB structure and how they could be observed in XAFS, describe in some detail the determination of the errors on the CN and extend the previous analysis to the higher coordination shells; in particular, we have performed a state-of-the-art *ab initio* analysis of the spectra including the important multiple-scattering (MS) contributions. This complete analysis is shown to be in agreement with the previously published first-shell analysis. We find no evidence of large reduction in CN's and our data is demonstrated to be compatible with the presence of a size effect, with nonreconstructed, incoherent, grain boundaries.

II. XAFS OF NANOPHASE MATERIALS

In this section we describe the effects on XAFS spectra of various possible structural models for n materials. A similar discussion relevant to XRD has been previously published by Löffler and Weissmüller,[17] and we follow that discussion closely, referring the reader to that paper for a complete justification of the formalism.

For the present discussion we neglect MS. The most general expression for the XAFS signal is[23,24]

$$\chi(k)=4\pi\int_0^\infty dr\ r^2\rho g_2(r)A(k,r)\sin\{2kr+\psi(k,r)\}, \tag{1}$$

where $g_2(r)$ is the two-body RDF, $A(k,r)$ is the amplitude, and $\psi(k,r)$ the phase shift. $A(k,r)$ includes thermal and structural damping terms, many-body correction factors and the $1/r^2$ term; the other symbols have their usual meaning. In the important case in which the total RDF can be split in a number of separate coordination shells then Eq. (1) becomes

$$\chi(k)=\sum_j N_j A(k,r_j)\sin\{2kr_j+\psi(k,r_j)\}, \tag{2}$$

where r_j and N_j are the average interatomic distance and the CN of the jth shell, respectively.

For a nanostructured material (be it an array of isolated clusters or a compacted nanophase) the RDF can be split in two terms: the intragrain contribution, deriving from those atomic correlations involving atoms belonging to the same particle, and the intergrain one, which derives from the remaining atomic correlations. It is useful then to introduce the intraparticle and interparticle correlation functions. The intraparticle correlation function $H(r)$ is the fraction of space contained within the same particle as the central atom in a spherical shell of radius r, averaged out with respect to all positions of the central atom inside the particle; the interparticle correlation function $H'(r)$ is defined analogously. The total RDF can then be written:

$$g_2(r)=g_2^v(r)H(r)+\langle g_2(r)\rangle^v H'(r), \tag{3}$$

where $g_2^v(r)$ is the RDF of an infinite ''reference'' crystal with the same atomic correlations as each particle and in the second term the average of the RDF over all particle orien-

tations $\langle g_2(r)\rangle^v$ multiplies the intergrain correlation function; we note that the quantity $\langle g_2(r)\rangle^v$ has no atomic-scale structure.

An important property of the intragrain correlation function $H(r)$ is that independent of the shape of the particles it has value unity at $r=0$ and an initial slope (for $r \ll D$, with D the particle size) proportional to the specific free-surface area of the particle. For a compacted nanophase:

$$H(r)=1-\frac{\alpha_{\mathrm{GB}}}{2}r \quad (r \ll D), \tag{4}$$

where, assuming sperical particles,

$$\alpha_{\mathrm{GB}}=\frac{3}{\langle D\rangle_A}; \tag{5}$$

α_{GB} is the specific GB area and $\langle D\rangle_A$ is the area-weighted average particle size. In the case of isolated particles the free-surface area is double so that the appropriate factor in Eq. (4) is $\alpha_S=2\alpha_{\mathrm{GB}}$.

We now substitute Eq. (3) in Eq. (1) for the XAFS to obtain

$$\chi(k)=4\pi\int_0^\infty dr\ r^2\rho g_2^v(r)H(r)A(k,r)\sin\{2kr+\psi(k,r)\}$$
$$+4\pi\int_0^\infty dr\ r^2\rho\langle g_2(r)\rangle^v H'(r)A(k,r)$$
$$\times\sin\{2kr+\psi(k,r)\}. \tag{6}$$

In this expression the second term does not contribute significantly to the structural signal since $\langle g_2(r)\rangle^v$ is essentially a smooth, increasing function of r with no atomic-scale structure. We conclude that XAFS, as wide-angle XRD, is insensitive to the distribution of interatomic spacings between atoms located in different grains. In fact, it is easy to see that an additional contribution to this insensitivity is the fact that XAFS is considerably less sensitive to medium and long-range correlations than XRD; this derives from the core-hole lifetime and to the absence of low k-space information. We now apply Eq. (6) to various limiting cases that will be useful in the discussion of the results.

A. Isolated nanometer-sized particles

This is the case encountered, for example, in the study of supported metal clusters:[25] each particle is effectively at an infinite distance from the others. The interparticle correlation function is zero except for distances very large compared to the interatomic distances and only the first term in Eq. (6) contributes to $\chi(k)$. If we separate the total $g(r)$ in coordination shells and analyze the first few, it is easy to see that, using the limit for $H(r)$ expressed by Eq. (4), each measured CN will be reduced by a factor $[1-(\alpha_S/4)r_j]$ with respect to the infinite reference structure; r_j is the interatomic distance of the jth shell.

B. Nanophase materials with nonreconstructed GB's

Upon compaction, isolated clusters will form a nanophase material. Atoms on the surface of each particle will now belong to the GB. If each atom in the neighborhood of the GB still occupies the lattice position of its original particle, i.e., if there are no atomic relaxations during the compaction process we refer to the GB's as "nonreconstructed," a term we borrow from surface science. Since, as explained above, the second term in Eq. (6) does not give any contribution, it is clear that in this case the first few coordination numbers will be reduced by a factor $[1-(\alpha_{\mathrm{GB}}/2)r_j]$.

C. Nanophase materials with disordered GB's

Upon compaction of isolated clusters and formation of a nanophase material the atoms in the GB's may undergo relaxations. If there is a large number of different local structures in which atoms are not on the lattice sites of the original particle, so that on the average there is no short-range order, we refer to the GB's as "disordered." It is easy to see that in this case the CN of the first few shells will be reduced by a factor of $x_L[1-(\alpha_{\mathrm{GB}}/2)r_j]$, where x_L is the fraction of atoms on lattice sites of the reference crystal. Compared to the case of nonreconstructed GB's, CN's are reduced by the extra factor x_L.

III. SAMPLE PREPARATION AND EXPERIMENTAL

Six samples of n-Pd were prepared by inert gas condensation with different treatments following the deposition. One sample (n.1) was not consolidated, in order to serve as a reference for an ensemble of clusters with a negligible grain-boundary density. All other samples were consolidated *in situ* under high vacuum for 5 to 10 min at 1–2 GPa; at this stage samples have a density from 84% to 87% of coarse-grained Pd. Following room-temperature consolidation, one sample was kept at liquid-nitrogen temperature (LNT) up to 1 week before measurement in order to reduce room-temperature (RT) grain growth. Two samples were stored at RT for different periods of time and the remaining two samples were subjected to annealing and hot-pressing procedures. No metallic impurities were detected in a scanning microprobe. Hot extraction on four samples yielded 0.6 ± 0.2 at. % O, 0.3 ± 0.1 at. % N, and 0.4 ± 0.3 at. % H.

The size distribution of materials prepared by inert gas evaporation has been proposed to be a log-normal distribution function.[26] For compacted materials, however, a bimodal distribution provides a better description, due to the details of the grain growth kinetics.[27] The particle size distribution functions, $n(D)$, for all our samples has been determined by indirect deconvolution of Bragg peaks.[27] The $n(D)$ curve for all compacted samples are shown in Fig. 1. For the uncompacted sample the determination of $n(D)$ was found to be unreliable. The area-weighted average grain size for each sample can be determined from these curves and it is listed in Table I, together with sample history. The rms strain values lie between 0.03% and 0.3%.

In order to perform XAFS experiments a thin ($\approx 10\ \mu$m), homogeneous sample is required; inhomogeneity in the sample thickness distribution is a major source of experimental artifact,[28,29] which may artificially reduce the measured coordination numbers; consequently, much care was devoted to this aspect. Notice that all known experimental artifacts tend to *reduce* the measured coordination num-

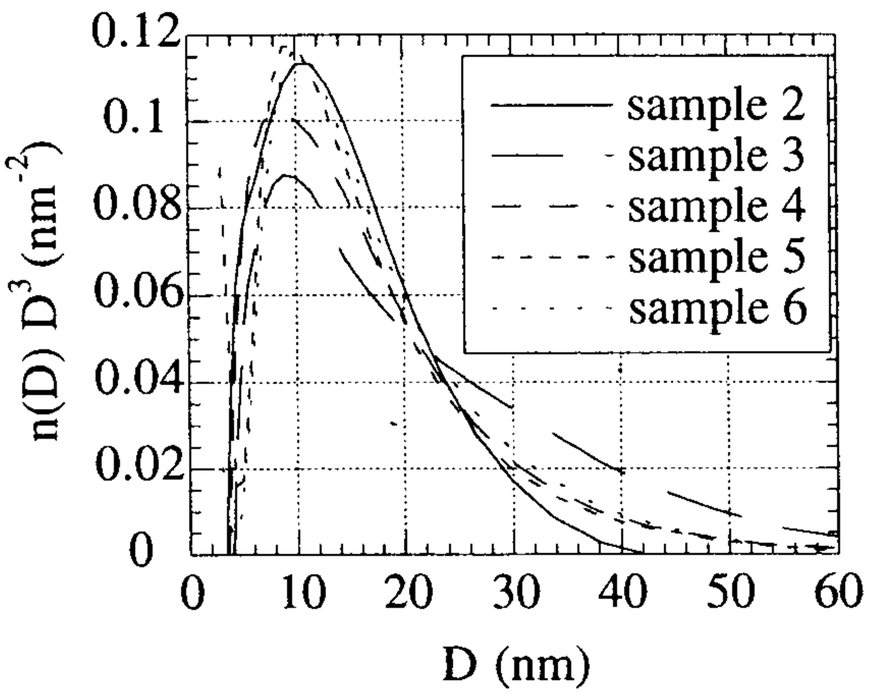

FIG. 1. Volume weighted particle size distributions for the compacted samples.

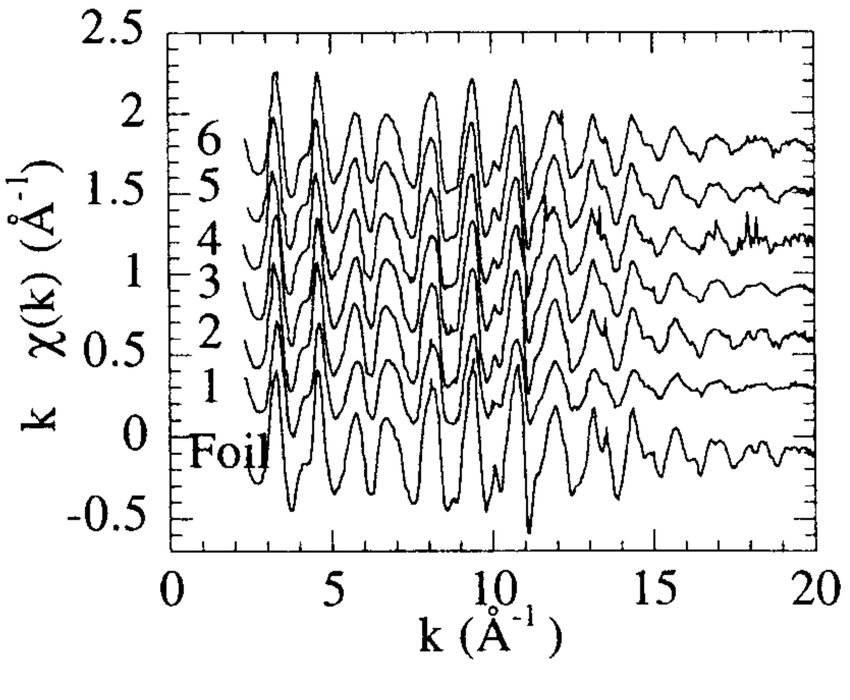

FIG. 2. Background subtracted XAFS functions for all samples and the coarse-grained foil.

bers, not to enhance them. The samples were lightly ball milled at LNT in order to produce a powder that was then dispersed in toluene using an ultrasound bath. Only the finest particles (those forming a fine suspension at the top of the test tube) were then deposited on a cellulose membrane forming a homogeneous sample. Homogeneity at the submicron level was checked optically and by measuring spectra on samples of different thicknesses, from 1 to 15 μm, which showed identical values of the CN's. We found that samples prepared by using all particles produced by ball milling (without dispersion in toluene and subsequent selection of finest particles) exhibited artificially reduced coordination numbers. In fact, samples of coarse-grained powder prepared in the same way showed the same artificially low coordination numbers. This experimental artifact might in part explain the previously reported low coordination numbers, at least on materials produced by inert gas evaporation.

XAFS measurements were performed on the GILDA CRG (D8) beamline of the European Synchrotron Radiation Facility, Grenoble, France. A Si(311) independent crystal monochromator with dynamical sagittal focusing[30] was used. Harmonics rejection was obtained by detuning the crystal using a closed-loop feedback controller; the absence of harmonics was checked with a hyperpure Ge solid-state detector and multichannel analyzer by measuring the elastically scattered radiation from the sample holder. XAFS spectra were measured in the transmission mode with Ar filled ionization chambers in the energy range 24–26 keV, with an energy resolution of 1.5 eV approximately; all spectra were measured at 77 K in order to reduce thermal damping of the signal and so increasing the available k space. For a few samples temperature-dependent measurements were performed and no variation of the determined average CN's was found, but only an increase of the thermal disorder factor in accordance to known vibrational behavior.[31] A coarse-grained Pd foil was measured as a reference sample.

TABLE I. Sample history and characteristics. $\langle D\rangle_A$ is the area-weighted average particle size.

Sample	Preparation/Treatment	$\langle D\rangle_A$
		(nm)
1	Not compacted	8.4
2	Stored at LNT	11.5
3	Stored at RT for 1 month	16.7
4	Stored at RT for 2 weeks	12.2
5	Hot pressed for 2 days 3.2 GPa, 100 °C	11.5
6	As No. 5, then annealed for 1 h at 160 °C	13.0

The background subtracted, raw XAFS functions, reaching 20 Å^{-1}, are reported in Fig. 2. These functions were Fourier transformed in the range 3–20 Å^{-1} and the magnitude of the Fourier transform is displayed in Fig. 3; no phase-shift correction has been applied. From the figures it is clear that the spectra show different amplitudes and can be roughly grouped in three sets in order of decreasing amplitude: the coarse-grained foil, samples 2 to 6 (i.e., all the compacted samples), and sample 1 (the uncompacted sample); clearly the analysis will have to reflect this qualitative trend. We note that the amplitude is the only apparent difference in the spectra; in particular there appear to be no changes in the interatomic distances.

The peaks in Fig. 3 correspond to interatomic correlations in the fcc structure of Pd. In a first approximation the major peaks are due to successive coordination shells (the first five are visible) with the interatomic distance scaling as the square root of the coordination shell order (in fact, this relation is true up to the thirteenth shell). Due to the presence of

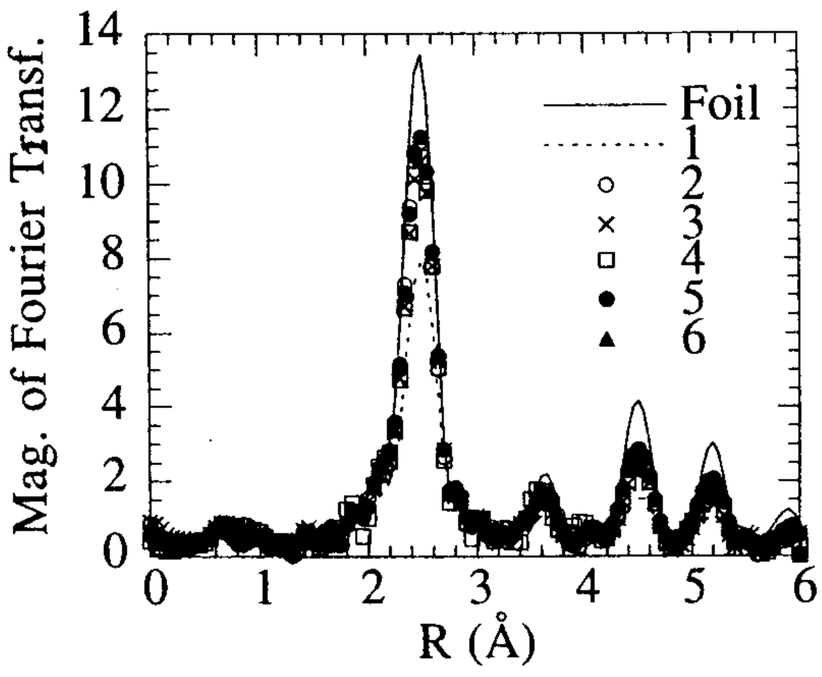

FIG. 3. Magnitude of the Fourier transform of the spectra presented in Fig. 2.

multiple scattering of the photoelectron, however, it is well known that atomic correlations of order higher than two contribute to the XAFS $\chi(k)$ function, the magnitude of the higher-order corrections depending on the specific system. This implies that, for the second coordination shell and above, a simple interpretation based on two-atom correlation can be a bad approximation; on the other hand, the lowest frequency signal due to the first coordination shell is only due to the two-body atom correlations and the single scattering (SS) theory of XAFS is applicable. In the fcc structure it is well known that the most important MS contribution arises from the collinear configuration of the nearest-neighbors and fourth shell atoms due to photoelectron focusing.[32]

IV. DATA ANALYSIS

The analysis of the spectra presented in the previous section was performed in two, complementary, steps. In the first step a conventional method based on Fourier filtering (FF) was applied in order to obtain local order parameters for the nearest neighbors (NN's). This implies the SS approximation which, as already noted, is valid for the lowest frequency contribution due to the NN's; moreover, the Fourier filtering technique is well tested and reliable for a simple structure such as the fcc and the extraction of local order parameters implies a simple four parameter fit. In order to analyze the higher-order shells the *ab initio* GNXAS program[33,34] was used; this program correctly treats the total contribution to the XAFS signal due to atomic correlations of second and third order using a method that is equivalent to including MS to any order. Using GNXAS (or other similar programs) to analyze the data is essential if one wants to correctly interpret signals due to higher-order shells.

A. Fourier filtering analysis of the first shell

Spectra were treated according to standard procedures. The pre-edge of the raw XAFS spectra was subtracted using a linear interpolation. A cubic spline fitted to the data was used in order to simulate the atomic cross section; the XAFS oscillations were then extracted by dividing the difference between the raw data and the spline by $J\times(1-\frac{8}{3}(E-E_0)/E_0)$ with J the jump height.[35] $\chi(k)$ functions were Fourier transformed in the range 3–20 Å^{-1}; an inverse Fourier transform was performed in the range 1.8–3.2 Å and the result is thus the SS signal from the NN atoms. This function was fitted to a model using the MINUIT (CERN) nonlinear least-squares routine with the following four free parameters: relative coordination number (N'), interatomic distance (r_l), variation of mean-square-relative-displacement ($\Delta\sigma^2$) and shift of threshold energy (ΔE_0); k^2 weighting of the data was used and the fitting range was 3.5–17 Å^{-1}. Experimental amplitudes and phases from the coarse-grained Pd foil were used as reference. The function minimized was

$$R=\frac{\Sigma(y_i-f_i)^2k_i^2}{\Sigma y_i^2k_i^2}, \tag{7}$$

where y_i are the data points and f_i are the corresponding fit points; typical values of R obtained were 5×10^{-3}. We note that the number of "independent data points" as defined in information theory[36] is $2\times\Delta R\times\Delta k/\pi=12$, so that with only four fitting parameters the fit is certainly significant.

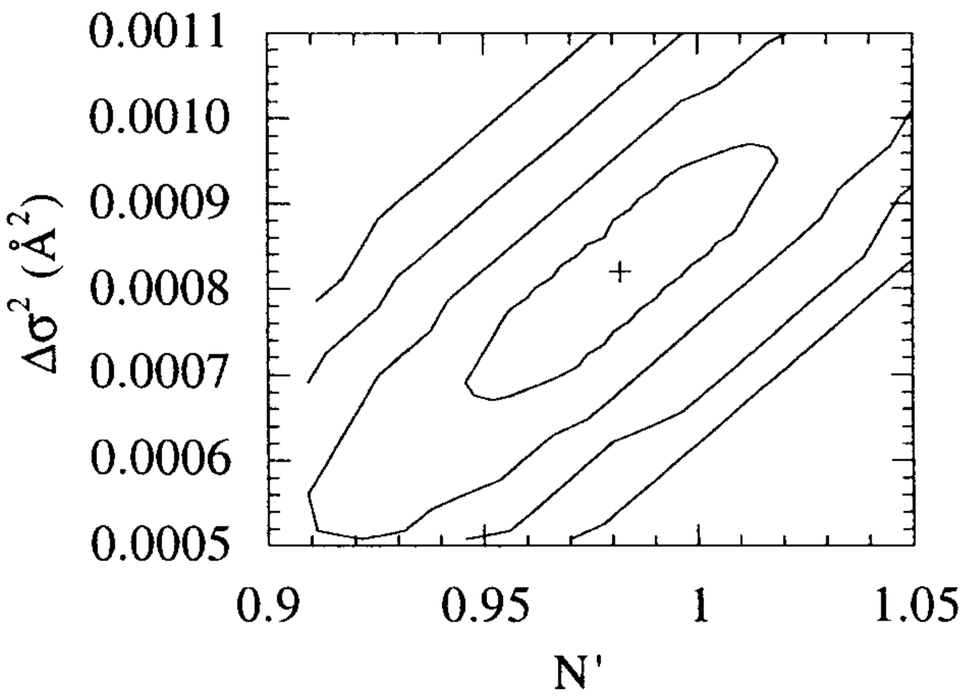

FIG. 4. Contour plot of the function R as a function of relative coordination number and variation of MSRD for sample 2, obtained with Fourier filtering analysis for the first shell. The inner ellipse encloses the 95% C.L. area; the first four contours are shown.

Since an accurate determination of the NN coordination number is of great importance, some care was devoted to the correct determination of the parameter errors. The main source of error in the determination of N' comes from correlation with $\Delta\sigma^2$. Error estimation was performed by plotting, as a function of $\Delta\sigma^2$ and N', contours of the function R at values $R_{\min}+U$, where $R_{\min}$ is the minimum of the fitting function and U determines the 95% confidence level for four fitting parameters.[37] This method takes into account the correlation between parameters and the area enclosed by the curve $R=R_{\min}+U$ is interpreted as that in which the parameters N' and $\Delta\sigma^2$ lie with 95% level probability. Such a contour is shown in Fig. 4 for sample 2. Contours of equal value of R are inclined ellipses, which graphically depicts the correlation between these two parameters. The error on one particular parameter can be found by projecting the extremes of the 95% C.L. ellipse on the relevant axis. For all samples these errors, which will be called 95% C.L. errors, were found to be 0.036 on N' and 0.16×10^{-3} Å^2 on $\Delta\sigma^2$. We note that it is more common to quote single parameter, one standard deviation errors (1σ-error); the $1-\sigma$ error is considerably smaller than the 95% C.L. error here adopted (in the present case the 1σ-error is 0.012 for N'); however, since the correct determination of the NN CN is crucial in this case, we adopt the conservative 95% C.L. error as the best determination of the statistical uncertainty on the parameter. We found that variations in the determination of the best value of each parameter due to different weightings and to slightly different filtering windows were within the 95% C.L. error.

Average NN CN's $\langle N^{(1)}\rangle_{\rm FF}=12\times N'$, and $\Delta\sigma^2_{\rm FF}$ values relative to the foil determined in this way are reported in Table II. An example of the fit for sample 2 is shown in Fig. 5. The interatomic distances in all nanophase samples were found to be identical to those of the coarse-grained reference.

The $\langle N^{(1)}\rangle_{\rm FF}$ and $\Delta\sigma^2_{\rm FF}$ values found in this analysis bear out the qualitative differences in the spectra referred to earlier. Samples 2 to 6 have $\langle N^{(1)}\rangle_{\rm FF}$ values between 11.5 and

TABLE II. First shell CN's and MSRD. Second and third column: as determined from Fourier filtering analysis; third and fourth column: as determined by GNXAS *ab initio* analysis; fourth and fifth column: estimates assuming nonreconstructed GB's, as described in the text.

Sample	$\Delta\sigma_1^2$ (10^{-3} Å^2)	$\langle N^{(1)}\rangle_{FF}$	σ_1^2 (10^{-3} Å^2)	$\langle N^{(1)}\rangle_{GNXAS}$	$N_\alpha^{(1)}$	$N_{n(D)}^{(1)}$
	($\pm$0.15)	($\pm$0.4)	($\pm$0.40)	($\pm$1.0)		
Foil	0, model	12, model	1.9	12, fixed		
1	1.20	9.7	3.0	9.6	11.41	11.33
2	0.80	11.7	2.4	11.4	11.57	11.50
3	0.90	11.5	3.1	11.0	11.70	11.60
4	1.00	12.0	2.4	11.5	11.59	11.52
5	0.70	11.8	2.4	11.3	11.57	11.50
6	0.80	12.0	2.4	11.6	11.62	11.57

12 $\Delta\sigma_{FF}^2$ ranging from 0.8 to 1.0×10^{-3} Å^{-2} while sample 1 has a significantly lower $\langle N_1\rangle_{FF}$ of 9.7 and slightly higher $\Delta\sigma_{FF}^2$.

B. *Ab initio* analysis

The GNXAS set of programs was used in order to perform an *ab initio* analysis of the spectra. Theoretical phase shifts were generated by using a nonoverlapping muffin-tin potential and a complex and energy-dependent Hedin-Lundquist self-energy term. A muffin-tin radius of 1 Å was used, but the exact value was not found to affect the results critically. By inspecting the fcc structure of Pd the interatomic correlations of order two and three (pair and triplet correlations) up to the eighth coordination shell were determined and appropriate atomic clusters constructed with the crystallographic coordinates of Pd. Theoretical XAFS signals and their derivatives with respect to the atomic coordinates due to these atomic correlations were then calculated using the continued fraction algorithm.[38] These theoretical signals were then used in a least-squares routine to fit the experimental spectra. Notice that the fitting is performed directly on the raw absorption data, with no Fourier filtering.

In order to determine the correct analysis procedure the spectrum of the coarse-grained foil was initially analyzed in detail. This step is necessary in order to identify the important contributions to the signal (and thus to avoid including those with negligible amplitude) and also to independently determine the value of the many-body amplitude reduction factor S_0^2 on a sample of known coordination number.

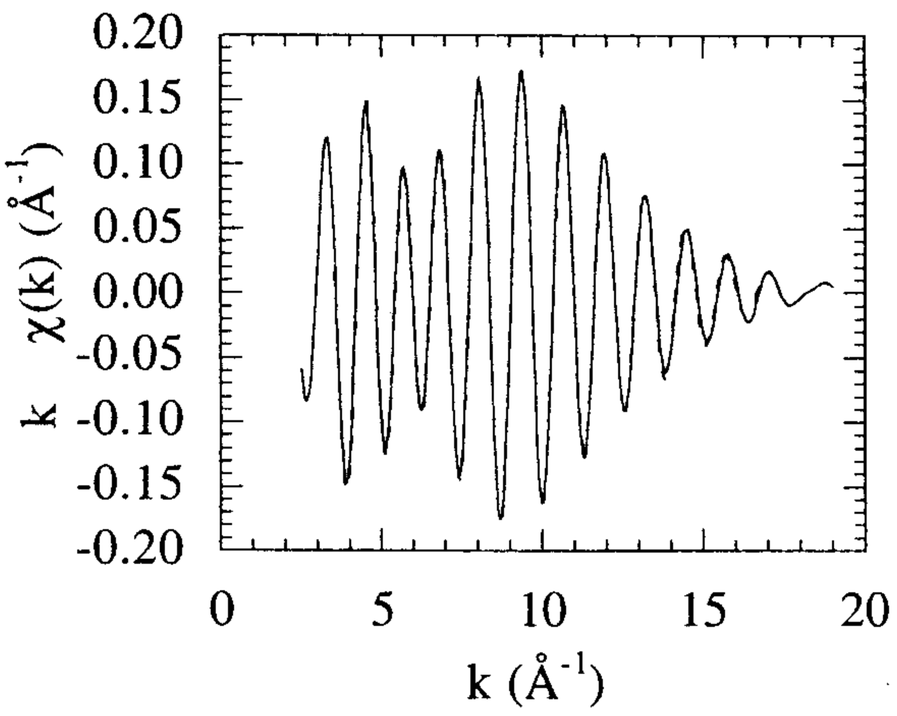

FIG. 5. Fit of the first-shell inverse Fourier transform for sample 2.

1. Analysis of the coarse-grained Pd foil

The atomic correlations which were found to give significant contributions to the XAFS signal and were included in the fitting were

(a) two-body correlations involving all coordination shells up to the eighth;

(b) three-body correlations involving: (i) 60° triangles linking NN's; (ii) 120° triangles linking central atom, first and third neighbors; (iii) collinear configurations of, on the one hand, first and fourth shell atoms and, on the other, second and eighth shell atoms.

Note that in the GNXAS methodology the third, fourth, and eighth shell two-body signals are generated from the atomic coordinates of the relevant three-body configurations.

Fitting of the spectrum was performed in the energy range corresponding to $k=3$ to 20 Å^{-1} with k^3 weighting by varying twelve parameters that can be divided in three groups: (a) interatomic distances: relative to the first, second, fifth, and seventh coordination shells (r_j); (b) damping terms: mean-square relative displacements of the first and second shells, a single MSRD value for the fifth, sixth, and seventh shells ($\sigma_{r_j}^2$), and bond-angle variance for the 120° triangles and the two collinear configurations ($\sigma_{\theta_j}^2$); (c) nonstructural parameters: many-body amplitude reduction factor (S_0^2) and energy threshold (E_0). The distance of the sixth shell was kept fixed at its crystallographic value as it was found to otherwise converge to an unphysical value, presumably due to the weakness of the signal. Off-diagonal elements in the matrix that describes damping of three-body contributions were fixed equal to 0 as it was found that they were affected by a very large error and that their exact value did not affect critically the fit. Since it is beyond the scope of this paper to discuss the analysis method in detail the reader is referred to the literature[33,34] for a full justification of the choice of fitting parameters and for a description of how they can be used to calculate all the important signals. Let us only note that although we are using a significant number of contributions fitting is performed with a relatively limited number of parameters (twelve).

The result of the fit is shown in Fig. 6(a): it is apparent that the experimental spectrum is reproduced very well by the fit; in Fig. 6(b) we show the Fourier transform of the

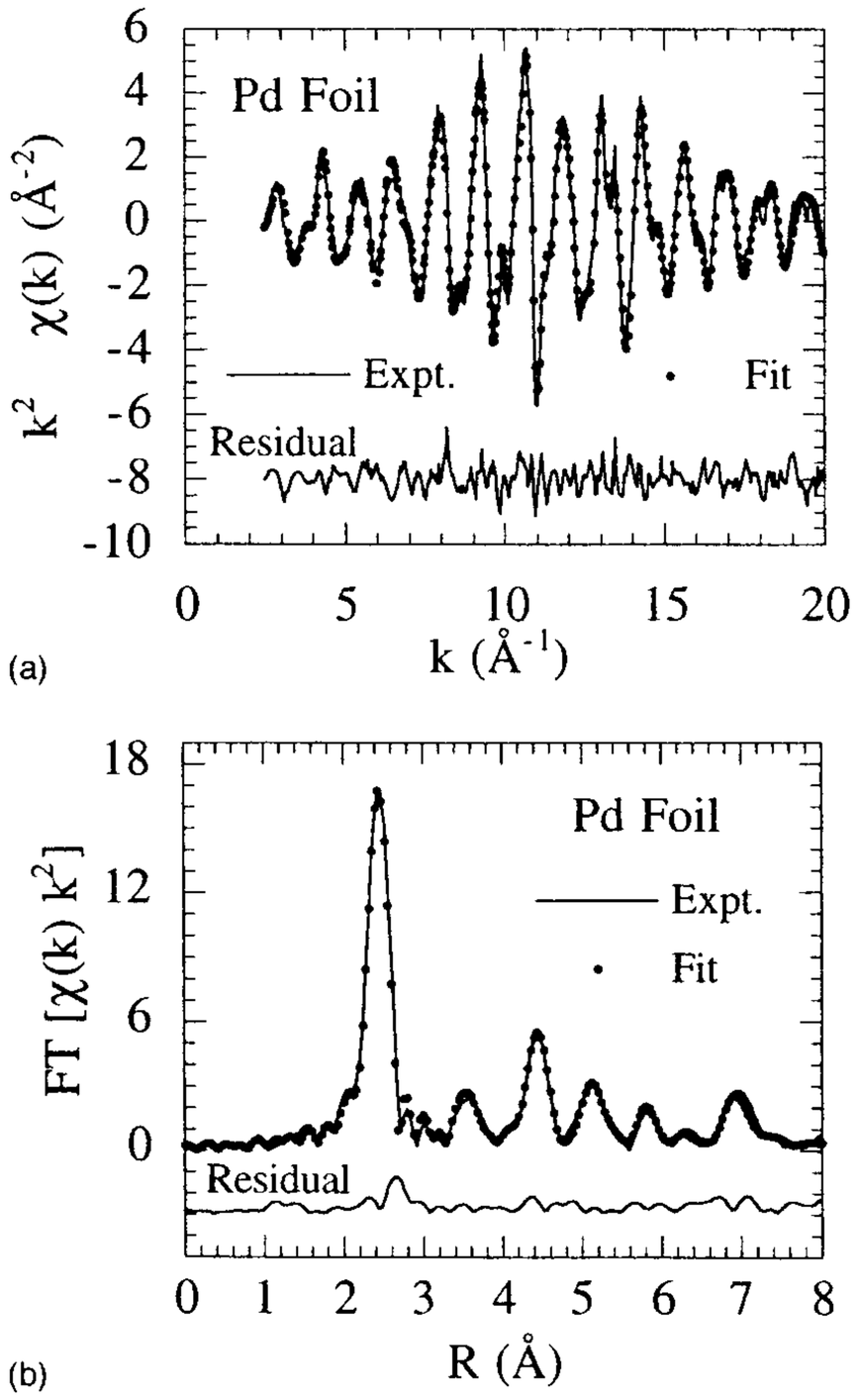

FIG. 6. (a) Fit of the full spectrum of the coarse-grained foil with GNXAS; also shown is the residual. (b) Fourier transform of the raw data, fit, and residual for the coarse-grained foil.

experiment, the fit, and the residual: in R space the comparison between fit and experiment is even more satisfying, with excellent agreement up to the eighth coordination shell.

The important parameters obtained from the fit are reported in Table III. It can be verified that there is excellent agreement between the crystallographic distances and those found; the error on the first-shell distance is noted to be very small. The value of S_0^2 has an 8% error, which is typical for *ab initio* determination of CN's. The values of $\sigma_{r_j}^2$ increase with r_j, indicating a gradual loss of correlation in atomic vibration.[31] Finally we note that bond-angle fluctuations are characterized by very large errors, due to the weakness of the associated signals.

2. First shell ab initio analysis

As a first step in the *ab initio* analysis of the nanophase samples and in order to compare results with the Fourier filtering technique the *ab initio* analysis was limited to the first shell. The full spectrum was fitted as already described for the foil but only the NN contribution was included; hence only four fitting parameters were used: r_1, $\sigma_{r_1}^2$, ΔE_0, and the average NN CN that we shall call $\langle N^{(1)} \rangle_{\text{GNXAS}}$ to distinguish it from $\langle N^{(1)} \rangle_{\text{FF}}$. The value of S_0^2 was fixed to that found for the foil.

No significant variation of r_1 with respect to the foil was found for any of the samples. Values of $\langle N^{(1)} \rangle_{\text{GNXAS}}$ and $\sigma_{r_1}^2$

TABLE III. Results of the GNXAS analysis of the coarse-grained Pd foil.

Parameter	Value	95% C.L. error
S_0^2	0.766	±0.062
r_1 (Å)	2.7452	±0.0030
r_2 (Å)	3.872	±0.013
r_3[a] (Å)	4.755	±0.0056
r_4[a] (Å)	5.490	±0.0060
r_5 (Å)	6.136	±0.023
r_6 (Å)	6.725, const	
r_7 (Å)	7.312	±0.020
r_8[a] (Å)	7.731	±0.026
$\sigma_{r_1}^2$ (10^{-3} Å^2)	1.92	±0.31
$\sigma_{r_2}^2$ (10^{-3} Å^2)	3.1	±1.2
$\sigma_{r_3}^{2\,a}$ (10^{-3} Å^2)	3.4	±1.3
$\sigma_{r_4}^{2\,a}$ (10^{-3} Å^2)	3.8	±0.62
$\sigma_{r_{5,6,7}}^2$ (10^{-3} Å^2)	4.4	±1.3
$\sigma_{r_8}^{2\,a}$ (10^{-3} Å^2)	6.3	±2.4
$\sigma_{\theta_{120}}^2$ (deg^2)	0.91	±1.4
$\sigma_{\theta_{180,1}}^2$ (deg^2)	1.6	±1.6
$\sigma_{\theta_{180,2}}^2$ (deg^2)	22	±29

[a]Two-body parameter obtained from triplet correlations.

are reported in Table II. Errors were determined as 95% C.L. errors, using the contour plot method. We note that errors using the *ab initio* analysis are significantly higher than with the Fourier filtering method. The numerical comparison with the results of the Fourier filtering analysis is good, with $\langle N^{(1)} \rangle_{\text{GNXAS}}$ being slightly lower than $\langle N^{(1)} \rangle_{\text{FF}}$ but within the errors. Also, the variation of $\sigma_{r_1}^2$ in the nanophase samples relative to the foil is found to be equal to the value of $\Delta\sigma_{r_1}^2$ determined by Fourier filtering, within the errors.

3. Ab initio multishell analysis

As described above, for an ensemble of randomly oriented particles and in the limit that the particle diameter is large with respect to the interatomic distance, the CN of each shell scales linearly with the interatomic distance of that shell:

$$N_j = N_{\text{ideal}}(1 - 0.5\alpha r_j), \tag{8}$$

where N_j is the CN of the jth shell, N_{ideal} is the CN of the same shell in the coarse-grained fcc foil, r_j is the interatomic distance for the jth shell and α depends on the IBR ratio of the sample. For a two-body signal Eq. (8) directly gives the reduction of the XAFS amplitude associated with each shell. For three-body signals one must consider the modification in the multiplicity, that is, the number of identical triangular configurations involving the excited atom and other two atoms in (possibly equal) given coordination shells. For a configuration with atoms in shells i and j the reduced multiplicity is

$$M_{ij} = M_{\text{ideal}}(1 - 0.5\alpha r_i)(1 - 0.5\alpha r_j). \tag{9}$$

If a fraction x_L of nonlattice atoms are present Eqs. (8) and (9) are modified by an additional factor x_L or x_L^2, respec-

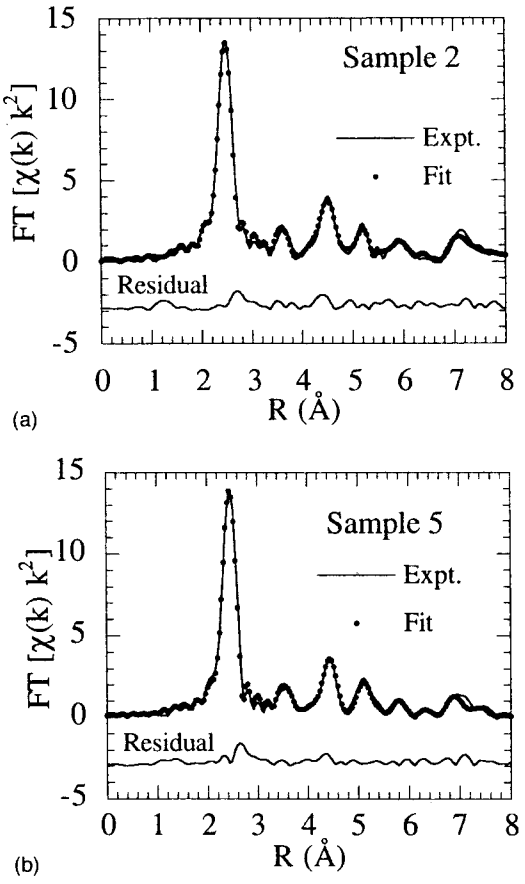

FIG. 7. Fourier transform of the raw data, of the fit with GNXAS, and of the residual for (a) sample 2 and (b) sample 5.

tively; for the moment this possibility will not be considered. The fitting routine was modified so that each two-body or three-body atomic correlation was weighed according to its expected reduced CN using the above equations.

We assumed nonreconstructed GB's and used α as a free parameter in fits of all the nanophase samples; together with α the other fitting parameters were those already described for the foil. The assumption of nonreconstructed GB's will be discussed in the next section. Examples of the fits thus obtained are shown, for samples 2 and 5, in Fig. 7: clearly this procedure reproduces extremely well the experiment. For all samples the values found for α are compatible with those obtained from the first-shell CN's listed in Table II by inverting Eq. (8) and with those found by analysis of the grain-size distribution (Table I). However, the determination of α is affected by a large error (as much as $\pm 60\%$); it was verified that this is due to the high correlation of these parameters with the damping terms and to the relative weakness of the contributions coming from the higher shells. The values of $\sigma_{r_j}^2$ are plotted in Fig. 8 as a function of interatomic distance. For all samples they show the same (very reasonable) qualitative behavior as for the foil, i.e., a gradual increase with r_j; all the nanophase samples show, however, higher values with respect to the foil, this difference also increasing with r_j.

The multishell analysis presented in this section demonstrates that the full XAFS spectrum can be reproduced very well assuming a nonreconstructed GB structure and is compatible with the NN CN's previously determined.

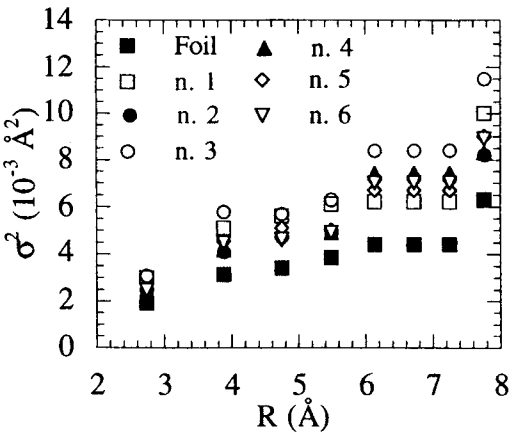

FIG. 8. Values of MSRD as a function of interatomic distance for all samples.

V. DISCUSSION

In this section we discuss the experimental evidence described above with particular reference to recent XRD measurements[17] and to the determination of the particle size distribution. We first of all concentrate on the NN data and then discuss the results on the higher shells.

The values of NN CN obtained by the two described analysis methods are listed in Table II and all the values lie between 11 and 12; if the more reliable Fourier filtering method is used the values lie between 11.5 and 12. We now compare this finding with two different methods to estimate the NN CN given the experimental particle size distribution and assuming nonreconstructed GB's. First of all, we have used Eq. (8) with $\alpha = 3/\langle D \rangle_A$ and $\langle D \rangle_A$ taken from Table I. The result is listed in Table II as $N_\alpha^{(1)}$. As an alternative estimate we have explicitly built a model of the fcc structure based on cubo-octahedrons; atoms on the surface have reduced coordination with respect to those in the bulk and the average coordination of a single particle constituted by n atomic layers around the central atom, $N(n)$, can be calculated[39] as

$$N(n) = \frac{40n^3 - 96n^2 + 80n - 24}{1/3(10n^3 - 15n^2 + 11n - 3)}. \tag{10}$$

The size D of the particle is taken to be twice the edge length, so that $D = 2r_1(n-1)$, where r_1 is the NN distance. The average coordination number for the ensemble was calculated as the volume weighted average of the particle size distribution $n(D)$ as determined by XRD:

$$N_{n(D)}^{(1)} = \int_0^\infty N(D) \times n(D) \times D^3 dD \Big/ \int_0^\infty n(D) \times D^3 dD. \tag{11}$$

Also in this second estimate the assumption is that the GB's are nonreconstructed; values of $N_{n(D)}^{(1)}$ are reported in Table II.

Experimental NN CN values for samples 2 to 6 are all quite close to both estimates. Clearly, the magnitude of the error puts some limits on what can be deduced from XAFS measurements alone. Specifically, the 95% C.L. error implies we can exclude neither the presence of 4% atoms off

lattice sites (on top of the decrease due to particle size) nor the case of full fcc coordination. We note that the case of full fcc coordination in the GB appears unreasonable as in this case the GB structure would only be a distorted version of the bulk. Notwithstanding the (small) uncertainties what the present analysis does demonstrate is that highly disordered GB's are not present. The reduction of NN CN for compacted materials can be simply explained by a size effect with no evidence of further reduction. Note that for the nonreconstructed case the reduction in CN for the atoms at the GB's is the same as that free surfaces. In terms of the concepts of order/disorder, that we adopted for the ease of discussion, this loss of coordination does not qualify as disorder. However, it does represent a quite dramatic change in local atomic short-range order relative to known homogeneously ordered (crystalline) or disordered (glassy) phases. The difference between nonreconstructed grain boundaries and free surfaces rests in the existence of intergrain atomic spacings at the former, but not at the latter. In an array of grains with random relative orientations the intergrain atomic spacings have a continuous distribution without peaks that cannot be resolved in the experiment. Compared to the crystal and to the relatively well-defined short- and medium-range order of most glasses this wide distribution constitutes a substantial loss of atomic positional correlation, hence of order.

The analysis of the higher coordination shells, performed with state-of-the-art methods, is compatible with the presence of nonreconstructed GB's. Justification for the use of this hypothesis in the multishell fits comes from the analysis of the first-shell data and also from XRD.[17] The fact that the full XAFS spectrum of all the samples can be fitted very well with this hypothesis provides further evidence for its validity and supports our previous first-shell report.[21]

The experimental evidence against the presence of a "disordered" GB component, already reported by us[21] and also by Stern *et al.* on *n*-Cu (Ref. 22) contradicts all previously published XAFS studies. The main difference of the work of Stern *et al.* with the present study is that surface sensitive electron yield detection was used; the near-surface grain-size distribution was not, however, determined and this may be different from that of the bulk. Common to the present work is the conclusion that "disordered" GB's are not present. The CN and MSRD for the sample kept at LNT were found to be identical, within the errors, with the values for the samples stored at room temperature. This indicates that either the low T storage was insufficient to prevent relaxation of the disordered as-prepared GB structure detected by x rays,[17] or that the preparation process specific to the XAFS experiment promoted relaxation, e.g., by removing microstructural mechanic constraints from the consolidation process.

Since previous XAFS work provided important support for the presence of a "disordered" GB component the present results must be considered in future models of GB structure. We have already discussed that for the samples deposited by inert gas evaporation at least a partial contribution to the enhanced reduction found in previous work may lie in sample thickness inhomogeneity. An XAFS study on *n*-Fe prepared by ball milling[20] has also found a very big (30 to 50%) reduction in NN CN; the particle size distribution was not, however, determined and the authors rely on an average value of the particle size, which might be misleading. Finally, we note that the improvements of sample preparation procedures over the last few years now provide well-characterized samples with regard to impurity content and particle size distribution.

The slight enhancement of all the $\sigma_{r_j}^2$ values with respect to the coarse-grained foil (as illustrated in Fig. 8) indicates that the process of evaporation and compaction produces a slight distortion of all the coordination shells. It is interesting to compare the present result with the determination of disorder by XRD, which is possible for the first shell. In the real-space analysis of XRD data[17] the slight increase of σ_1^2 was not resolved. However, we believe that the present results are more reliable as a greater portion of reciprocal space is probed by XAFS ($6-40\ \text{Å}^{-1}$) than by XRD ($0.3-17.3\ \text{Å}^{-1}$) and because the present analysis avoids the approximations involved in fitting the truncation-broadened peaks in the x-ray atomic distribution function by Gaussians; note also that the temperatures of the experiments are different, so that the absolute values of σ are not directly comparable. In a k-space analysis of XRD (Ref. 40) an (isotropic) increase of $3\times10^{-3}\ \text{Å}^2$ in the mean-square displacement (MSD) was found, to be compared with the $0.8\times10^{-3}\ \text{Å}^2$ we find for the increase in MSRD; in this case the two techniques measure different quantities, XAFS being sensitive to the relative atomic displacements (hence only to uncorrelated atomic displacements) while XRD measures the atomic displacements from the lattice positions. By comparing the numerical results of the two techniques we conclude that the increase in MSD is due in the most part to atomic displacements which are correlated in first coordination shell. The slight increase in $\sigma_{r_j}^2$ may have both a structural and a dynamic component,[41] which cannot be decoupled from the present measurements alone. The small reduction of σ_1^2 upon compaction indicates that atoms in the outermost layer of each crystallite have greater constraints of motion in grain boundaries than on a free cluster surfaces and/or reduced static disorder.

Sample 1 (with a negligible grain-boundary density) shows greatly reduced CN's for all shells. Since this sample has not been compacted the only possible origin for this is the high IBR; we note that a reduction of CN's has been previously reported in XAFS studies of metallic clusters.[41] The fact that all CN's increase upon compaction is clear evidence for particle aggregation. Unfortunately, the particle size distribution for sample 1 is not reliable so it is not possible to determine whether compaction is also accompanied by a change in particle size distribution that justifies the variation of CN's within the model of nonreconstructed GB's; this would be important in order to assess whether compaction produces structural rearrangement for the atoms in the near surface or GB regions. A result similar to the one reported here has been previously published[42] but no analysis or explanation had been given; also, different detection techniques were used for the uncompacted and the compacted samples, possibly causing systematic errors.

In conclusion, we have reported a comprehensive investigation of nanophase palladium by x-ray-absorption spectros-

copy with the aim of clarifying the issue of the structure of the grain boundaries in nanophase materials. Contrary to previous reports we find that the reduction in average coordination numbers is smaller than previously reported (at most 4 $\pm 0.03\%$ for the first shell) and can be explained by a size effect due to the non-negligible interface-to-bulk ratio of the samples. The analysis of the x-ray-absorption data has been extended up to the eighth coordination shell taking into account the important multiple-scattering paths.

ACKNOWLEDGMENTS

F.B. is grateful for hospitality at ESRF during the period in which this paper was written. We are grateful to A. Di Cicco and A. Filipponi for discussions on the GNXAS method. This work was supported by DFG (SFB277). XAFS measurements were performed at the European Synchrotron Radiation Facility, BP 220, F-38043 Grenoble CEDEX, France, within the public user program.

*Corresponding author; Electronic address: boscherini@lnf.infn.it
†Present address: ESRF, BP 220, F-38043, Grenoble CEDEX, France.

[1] H. Gleiter, in *Second Risó International Symposium on Metallurgy and Materials Science*, edited by N. Hansen, T. Leffers, and H. Lilholt (Risó National Lab., Røskilde, Denmark, 1981), pp. 15–21.
[2] H. Gleiter, Prog. Mater. Sci. **33**, 223 (1989).
[3] R. Siegel, Mater. Res. Soc. Bull. **XV**, 60 (1990).
[4] X. Zhu, R. Birringer, U. Herr, and H. Gleiter, Phys. Rev. B **35**, 9085 (1987).
[5] M. R. Fitzsimmons, J. A. Eastman, M. Muller-Stach, and G. Wallner, Phys. Rev. B **44**, 2452 (1991).
[6] J. Weissmüller, R. Birringer, and H. Gleiter, in *Microcomposite and Nanophase Materials*, edited by D. C. Van Acken, G. S. Was, and A. K. Gosh (TMS, Warrendale, PA, 1991), pp. 1–14.
[7] G. J. Thomas, R. W. Siegel, and J. A. Eastman, Scr. Metall. Mater. **24**, 201 (1990).
[8] E. Jorra, H. Franz, J. Peisl, G. Wallner, W. Petry, R. Birringer, H. Gleiter, and T. Haubold, Philos. Mag. B **60**, 159 (1989).
[9] P. G. Sanders, J. R. Weertman, J. G. Barker, and R. W. Siegel, Scr. Metall. Mater. **29**, 91 (1993).
[10] U. Herr, J. Jing, U. Gonser, and H. Gleiter, Solid State Commun. **76**, 197 (1990).
[11] S. Trapp, C. T. Limbach, U. Gonser, S. J. Campbell, and H. Gleiter, Phys. Rev. Lett. **75**, 3760 (1995).
[12] H. E. Schaefer, in *Mechanical Properties and Deformation Behavior of Materials Having Ultra-fine Microstructure*, edited by M. Nastasi, D. M. Parkin, and H. Gleiter (Kluwer, Amsterdam, 1993).
[13] D. Wolf and J. F. Lutsko, Phys. Rev. Lett. **60**, 1170 (1988).
[14] D. Wolf, Acta Metall. **37**, 2823 (1989).
[15] D. Wolf, Acta Metall. **37**, 1983 (1989).
[16] J. Wang, D. Wolf, S. R. Phillpot, and H. Gleiter, Philos. Mag. A **73**, 517 (1996).
[17] J. Löffler and J. Weissmüller, Phys. Rev. B **52**, 7076 (1995).
[18] D. C. Koningsberger and R. Prins, *X-Ray Absorption* (Wiley, New York, 1988).
[19] F. Boscherini, in *Fundamental Properties of Nanostructured Materials*, edited by D. Fiorani and G. Sberveglieri (World Scientific, Singapore, 1994), pp. 88–98.
[20] A. Di Cicco, M. Berrettoni, S. Stizza, E. Bonetti, and G. Cocco, Phys. Rev. B **50**, 12 386 (1994).
[21] S. de Panfilis, F. D'Acapito, V. Haas, H. Konrad, J. Weissmüller, and F. Boscherini, Phys. Lett. A **207**, 397 (1995).
[22] E. A. Stern, R. W. Siegel, M. Newville, P. G. Sanders, and D. Haskel, Phys. Rev. Lett. **75**, 3874 (1995).
[23] A. Filipponi, J. Phys.: Condens. Matter **6**, 8415 (1994).
[24] S. Mobilio and L. Incoccia, Nuovo Cimento D **3**, 846 (1984).
[25] A. Pinto, A. R. Pennisi, G. Faraci, G. D'Agostino, S. Mobilio, and F. Boscherini, Phys. Rev. B **51**, 5315 (1995).
[26] C. G. Granqvist and R. A. Buhrman, J. Appl. Phys. **47**, 2200 (1976).
[27] J. Weissmüller, J. Löffler, C. E. Krill, and R. Birringer (unpublished).
[28] E. Stern and K. Kim, Phys. Rev. B **23**, 1981 (1981).
[29] J. Goulon, C. Goulon Ginet, R. Cortes, and M. Dubois, J. Phys. (Paris) **43**, 539 (1982).
[30] S. Pascarelli, F. Boscherini, F. D'Acapito, J. Hrdy, C. Meneghini, and S. Mobilio, J. Synchrotron Radiat. **3**, 147 (1996).
[31] G. Beni and P. M. Platzman, Phys. Rev. B **14**, 1514 (1976).
[32] P. A. Lee and J. B. Pendry, Phys. Rev. B **11**, 2795 (1975).
[33] A. Filipponi and A. DiCicco, Phys. Rev. B **52**, 15 135 (1995).
[34] A. Filipponi, A. Di Cicco, and C. R. Natoli, Phys. Rev. B **52**, 15 122 (1995).
[35] P. Eisenberger and B. Lengeler, Phys. Rev. B **22**, 3551 (1980).
[36] P. A. Lee, P. H. Citrin, P. Eisenberger, and B. M. Kincaid, Rev. Mod. Phys. **53**, 769 (1981).
[37] W. H. Press, S. A. Teulosky, W. T. Vetterling, and B. P. Flannery, *Numerical Recipes* (Cambridge University Press, New York, 1992).
[38] A. Filipponi, J. Phys.: Condens. Matter **3**, 6489 (1991).
[39] A. Khoutami, B. Legrand, C. Mottet, and G. Tréglia, Surf. Sci. **307-309**, 735 (1994).
[40] J. A. Eastman, M. R. Fitzsimmons, and L. J. Thompson, Philos. Mag. B **66**, 667 (1992).
[41] A. Balerna and S. Mobilio, Phys. Rev. B **34**, 2293 (1986).
[42] J. A. Eastman, M. R. Fitzsimmons, M. Müller-Stach, G. Wallner, and W. T. Elam, Nanostruct. Mater. **1**, 47 (1992).